0026-895X/00/050936-10$3.00/0
MOLECULAR PHARMACOLOGY
Copyright © 2000 The American Society for Pharmacology and Experimental Therapeutics
Mol Pharmacol 58:936–945, 2000

Vol. 58, No. 5
70/860041
Printed in U.S.A.

Characterization of Calcium Signaling by Purinergic Receptor-Channels Expressed in Excitable Cells

TAKA-AKI KOSHIMIZU, FREDRICK VAN GOOR, MELANIJA TOMIĆ, ANDERSON ON-LAM WONG, AKITO TANOUE, GOZOH TSUJIMOTO, and STANKO S. STOJILKOVIC

Endocrinology and Reproduction Research Branch, National Institute of Child Health and Human Development, National Institutes of Health, Bethesda, Maryland (T.K., F.V.G., M.T., A.O.-L.W., S.S.S.); and Department of Molecular Cellular Pharmacology, National Children's Medical Research Center, Tokyo, Japan (A.K., G.T.)

Received February 4, 2000; accepted July 17, 2000

This paper is available online at http://www.molpharm.org

ABSTRACT

ATP-gated purinergic receptors (P2XRs) are a family of cation-permeable channels that conduct Ca^{2+} and facilitate voltage-sensitive Ca^{2+} entry in excitable cells. To study Ca^{2+} signaling by P2XRs and its dependence on voltage-sensitive Ca^{2+} influx, we expressed eight cloned P2XR subtypes individually in gonadotropin-releasing hormone-secreting neurons. In all cases, ATP evoked an inward current and a rise in $[Ca^{2+}]_i$. P2XR subtypes differed in the peak amplitude of $[Ca^{2+}]_i$ response independently of the level of receptor expression, with the following order: $P2X_1R < P2X_3R < P2X_4R < P2X_{2b}R < P2X_{2a}R < P2X_7R$. During prolonged agonist stimulation, Ca^{2+} signals desensitized with different rates: $P2X_3R > P2X_1R > P2X_{2b}R > P2X_4R \gg P2X_{2a}R \gg P2X_7R$. The pattern of $[Ca^{2+}]_i$ response for each P2XR subtype was highly comparable with that of the depolarizing current, but the activation and desensitization rates were faster for the current than for $[Ca^{2+}]_i$. The $P2X_1R$, $P2X_3R$, and $P2X_4R$-derived $[Ca^{2+}]_i$ signals were predominantly dependent on activation of voltage-sensitive Ca^{2+} influx, both voltage-sensitive and -insensitive Ca^{2+} entry pathways equally contributed to $[Ca^{2+}]_i$ responses in $P2X_{2a}R$- and $P2X_{2b}R$-expressing cells, and $P2X_7R$ operated as a nonselective pore capable of conducting larger amounts of Ca^{2+} independently on the status of voltage-gated Ca^{2+} channels. Thus, Ca^{2+} signaling by homomeric P2XRs expressed in an excitable cell is subtype-specific, which provides an effective mechanism for generating variable $[Ca^{2+}]_i$ patterns in response to a common agonist.

ATP-gated purinergic receptor-channels (P2XRs) are expressed in the central and peripheral nervous systems and in neuroendocrine and endocrine cells (Ralevic and Burnstock, 1998), including those of the pituitary gland (Koshimizu et al., 1998a,b). Activation of P2XRs evokes an inward current that is associated with membrane depolarization and an elevation in intracellular free calcium concentration ($[Ca^{2+}]_i$). In excitable cells, Ca^{2+} influx through the pore of these channels accounts in part for the increase in $[Ca^{2+}]_i$, the rest occurring indirectly through voltage-gated Ca^{2+} channels. The elevation of $[Ca^{2+}]_i$ by P2XR participates in the control of a number of cellular functions, such as neurotransmission and hormone secretion (Brake and Julius, 1996; North, 1996). Expression, cloning, and homology screening of cDNA for P2XRs revealed the presence of a family of seven subunits (denoted $P2X_xR$; $x = 1$ to 7) and several spliced variants (Brake et al., 1994; Bo et al., 1995; Chen et al., 1995; Lewis et al., 1995; Collo et al., 1996; Garcia-Guzman et al., 1996; Soto et al., 1996; Brandle et al., 1997; Rassendren et al., 1997). They have little primary sequence homology to other ligand-gated channels (Buell et al., 1996). Each subunit is proposed to have two transmembrane domains connected with a large extracellular loop, with both the amino- and carboxyl-termini located in the cytoplasm. The subunits have 35 to 59% amino acid homology and all of them can form cation-permeable pores when expressed in *Xenopus laevis* oocytes or in mammalian cells (Buell et al., 1996).

The temporal pattern and extent of Ca^{2+} entry plays a key role in the course of $[Ca^{2+}]_i$ signaling generated by P2XRs. However, relative contribution of the voltage-sensitive Ca^{2+} influx to the P2XR-induced Ca^{2+} signaling has been incompletely characterized. Some P2XRs are more permeable to Ca^{2+} ions than they are to monovalent cations, with a relative permeability of Ca^{2+} to Na^+ of about 4:1 (Evans et al., 1996). This finding suggests that the Ca^{2+}-conducting capability of P2XRs, like that of NMDA-type glutamate receptors, is more important, as are their roles in controlling electrical activity and voltage-sensitive Ca^{2+} influx (Hille, 1991). Such a hypothesis also explains how P2XRs generate Ca^{2+} signals when expressed in nonexcitable cells. On the other hand, in physiological conditions only a fraction of the total current

ABBREVIATIONS: P2XRs, purinergic receptor-channels; GT1 cells, gonadotropin-releasing hormone-secreting neurons; GFP, green fluorescence protein; HA, hemagglutinin; BzATP, 3′-*O*-(4-benzoyl)benzoyl-ATP.

through P2XR pores (between 6 and 15%) is carried by Ca^{2+}, because extracellular Ca^{2+} is lower than Na^{+} (Brake and Julius, 1996; North, 1996). This suggests that the capacity of these receptors to directly generate Ca^{2+} signals is limited. Furthermore, activation of P2XRs is frequently accompanied with their desensitization, the rate of which is intrinsic to the composition of channel subunits. Fast desensitization effectively abolishes current response within seconds of exposure to ATP (Chen et al., 1995; Lewis et al., 1995; North, 1996). The impact of the receptor desensitization to the voltage-insensitive and voltage-sensitive Ca^{2+} influx has not been studied extensively in a subtype specific manner. This emphasized the need for a study on current and Ca^{2+} signaling by recombinant P2XRs expressed in excitable mammalian cells.

Here, we examined the pattern of Ca^{2+} signaling evoked by all P2XRs in the presence and absence of voltage-gated Ca^{2+} channel activity. To do this, we expressed recombinant P2XRs in immortalized gonadotropin-releasing hormone-secreting GT1–7 neurons (hereafter GT1 cells). Like many neuroendocrine and endocrine cells, GT1 cells exhibits spontaneous action potential-driven Ca^{2+} entry through T- and L-type voltage-gated calcium channels (Van Goor et al., 1999a,b). Furthermore, neither P2XRs nor the calcium-mobilizing P2Y receptors are native to GT1 cells (Koshimizu et al., 1998b), in contrast to many other immortalized cells that are commonly used for transfection studies. Therefore, these cells are an excellent mammalian model system to analyze Ca^{2+} signaling by P2XRs and its dependence on voltage-sensitive Ca^{2+} influx. Our study focuses on the comparison of current and Ca^{2+} signaling by different homomeric P2XRs in GT1 cells and on the dependence of Ca^{2+} signaling on the voltage-sensitive Ca^{2+} influx.

Experimental Procedures

Cell Cultures and Transfection. GT1 cells were cultured in Dulbecco's modified Eagle's medium/Ham's F12 medium (1:1) containing 10% (v/v) fetal bovine serum, 100 μg/ml streptomycin, and 100 U/ml penicillin. Procedures for transient transfection in GT1 cells and expression constructs used were described (Koshimizu et al., 1999) with minor modifications. Briefly, cells were plated on coverslips coated with poly-L-lysine at a density of 0.5 to 1.0 $\times$ 10^5 cell/35-mm dish and allowed to grow for 24 h. On the following day, 1.2 to 2.5 μg of expression constructs encoding P2XRs was mixed with 8 μl of Lipofectamine in 1.2 ml of Opti-MEM (both from Life Technologies, Rockville, MD) for 15 to 20 min at ambient temperature. The DNA mixture was then applied to cells for 3 to 6 h and replaced by normal culture medium. Cells were subjected to experiments 24 to 48 h after transfection.

Stable Transfection of $P2X_1R$, $P2X_{2a}R$, and $P2X_{2b}R$. For stable transfection, cDNAs with the full-length coding sequence of $P2X_1R$, $P2X_{2a}R$, and $P2X_{2b}R$ were subcloned into the eukaryotic expression vector pcDNA 3.1/Zeo (Invitrogen, Carlsbad, CA). After transfection with Lipofectamine, stably transfected cell colonies were isolated by zeocin selection (400 μg/ml; Invitrogen) for at least 6 weeks. Reverse transcription-polymerase chain reaction, using primers flanking the coding sequence of respective receptors, verified expression of P2XR mRNAs in these cells. Functional expression of P2XRs were also confirmed by increases in $[Ca^{2+}]_i$ after challenging the cells with 100 μM ATP. In these studies, GT1 cells transfected with an empty vector without insert were used as the negative control and did not exhibit any $[Ca^{2+}]_i$ responses after ATP stimulation.

$[Ca^{2+}]_i$ Measurements. Cells were incubated at 37°C for 60 min with 1 μM fura-2 AM in phenol red- and ATP-free DMEM and subsequently washed with assay buffer containing 137 mM NaCl, 5 mM KCl, 1.2 mM $CaCl_2$, 1 mM $MgCl_2$, 10 mM HEPES, and 10 mM glucose. Cultures were kept for at least 30 min in this medium before single-cell $[Ca^{2+}]_i$ measurements. Apyrase (grade I) was purchased from Sigma (St. Louis, MO) and used at 20 μg/ml throughout the incubation process indicated. Coverslips with cells were mounted on the stage of an Axiovert 135 microscope (Carl Zeiss, Oberkochen, Germany) attached to the Attofluor Digital Fluorescence Microscopy System (Atto Instruments, Rockville, MD). $[Ca^{2+}]_i$ responses were examined under a 40$\times$ oil immersion objective during exposure to alternating 340 and 380 nm light beams, and the intensity of light emission at 520 nm was measured. The ratio of light intensities, F_{340}/F_{380}, which reflects changes in $[Ca^{2+}]_i$, was simultaneously followed in several single cells.

Use of GFP as a Marker for Cells with P2XR Expression. To characterize the transfection efficiency in single cells and to analyze the dependence of the pattern of Ca^{2+} response on expression efficiency, transfected GT1 cells with P2XR were identified from total cell population using green fluorescence protein (GFP) as a marker. Plasmid constructs for the simultaneous expression of GFP and P2XR in transfected cells was achieved either by subcloning the coding sequence of P2XR into a bicistronic GFP-expression vector $pIRES_2$-EGFP (Clontech, Palo Alto, CA), or by cotransfection of P2XR expression vector with a GFP-expression vector $pEGFP\text{-}C_1$ (Clontech) at ratio of 5:1. Cells expressing fluorescence protein were optically detected by an emission signal at 520 nm when excited by 488-nm light, and were not detectable by 340- or 380-nm excitations. We thus considered the emission signal from fluorescence protein by 340- or 380-nm excitations being within our background level for fura-2 measurements. The GFP intensity was recorded before $[Ca^{2+}]_i$ measurements and was expressed in arbitrary units (0 to 100). About 90% of GFP-positive cells responded with a rise in $[Ca^{2+}]_i$ after addition of 100 μM ATP.

Immunological Detection of C-Terminally Tagged P2XRs. Hemagglutinin epitope (HA; YPYDVPDYA) was inserted after a glycine residue next to the last amino acid of each receptor polypeptide by polymerase chain reaction. The 3′-primer sequence contained six bases of *Eco*RI site, three bases for stop codon, 27 bases encoding the nine amino acid HA-peptide sequence, three bases for glycine, and 21 bases encoding the seven amino acids next to the stop codon. The 5′-primer sites were chosen from the receptor coding sequences. The resulting HA-tagged P2XR fragments were subcloned into pBluescript II (Stratagene, La Jolla, CA) for sequencing. The correctly tagged C-terminal fragment was digested with *Eco*RI and *Eco*RV ($P2X_1R$), *Bsp*EI ($P2X_{2a}R$, $P2X_{2b}R$, and $P2X_7R$), or *Xho*I ($P2X_3R$), gel-purified, and ligated to the corresponding sites of the expression constructs.

Protein samples for Western blot were prepared from GT1 cells 24 h after transient transfection. Cells in a 100-mm dish were rinsed with ice-cold PBS and collected in TE buffer (50 mM Tris·HCl, pH 7.4, containing 5 mM EDTA, 10 μg/ml aprotinin, 10 μg/ml leupeptin, and 0.1 mM phenylmethylsulfonyl fluoride). Cells were homogenized on ice and crude membrane fractions were collected by centrifugation at 10,000*g* for 30 min at 4°C. The resultant pellet (about 1 mg protein) was resuspended in the same buffer for SDS-polyacrylamide gel electrophoresis (PAGE) (10 μg protein/lane). After electrophoresis, size-fractionated proteins were transferred to polyvinylidene fluoride membranes by electroblotting. The blots were incubated in 3% bovine serum albumin in TBS (10 mM Tris-Cl, pH 7.5, and 150 mM NaCl), followed by monoclonal anti-HA antibody (BAbCo, Richmond, CA) at a dilution of 1:3,500. After that, positive signals of individual blots were visualized by incubating the membrane with peroxidase-conjugated anti-mouse antibody (1: 5,000) and subsequent treatment with enhanced chemiluminescence Western blotting detection reagents (Amersham-Pharmacia, Arlington Heights, IL). Protein concentrations in the samples for Western blot were

determined using a Pierce BCA protein assay kit (Pierce, Rockford, IL).

Electrophysiological Recordings. Ionic currents and membrane potential (V_m) were measured using the perforated-patch recording technique (Rae et al., 1991). Current- and voltage-clamp recordings were performed at room temperature using an Axopatch 200 B patch-clamp amplifier (Axon Instruments, Foster City, CA) and were low-pass filtered at 2 kHz. Patch pipette tips (3–5 MΩ) were briefly immersed in amphotericin B-free solution and then back-filled with amphotericin B (240 μg/ml)-containing solution. Before seal formation, liquid junction potentials were canceled. An average series resistance of 17 ± 1 MΩ was reached 10 min following the formation of a GΩ seal (seal resistance > 5 GΩ) and remained stable for up to 1 h. Data acquisition and analysis were performed using a PC equipped with a Digidata 1200 A/D interface in conjunction with Clampex 8 (Axon Instruments). Unless otherwise stated, all ATP-induced currents were evoked in cells held at −90 mV.

Simultaneous Measurement of $[Ca^{2+}]_i$ and Current or V_m. GT1 neurons were incubated for 30 min at 37°C in phenol red-free medium 199 containing Hanks' salts, 20 mM sodium bicarbonate, 20 mM HEPES and 0.5 μM indo-1 AM (Molecular Probes, Eugene, OR). Coverslips with cells were then washed twice with modified Krebs-Ringer's solution containing 120 mM NaCl, 4.7 mM KCl, 2.6 mM $CaCl_2$, 2 mM $MgCl_2$, 0.7 mM $MgSO_4$, 10 mM HEPES, 10 mM glucose (pH adjusted to 7.4 with NaOH) and mounted on the stage of an inverted epifluorescence microscope (Nikon, Tokyo, Japan). A photon counter system (Nikon) was used to simultaneously measure the intensity of light emitted at 405 nm and at 480 nm after excitation at 340 nm. Background intensity at each emission wavelength was corrected. Perforated patch recording techniques (see above) were used to monitor current or V_m. The data were digitized at 4 kHz using a PC equipped with the Clampex 8-software package in conjunction with a Digidata 1200 A/D converter (Axon Instruments).

Solutions. Unless otherwise specified, the bath solution contained modified Krebs-Ringer salts and the pipette solution contained 70 mM KCl, 70 mM K-aspartate, 1 mM $MgCl_2$, and 10 mM HEPES (pH adjusted to 7.2 with KOH). Because of the inhibitory actions of divalent cations on $P2X_7R$, their activation by ATP was recorded in the presence of modified Krebs-Ringer salts without the addition of $MgCl_2$ and with 0.5 mM $CaCl_2$. All reported V_m values were corrected for a liquid junction potential between the pipette and a bath solution of +10 mV (Barry, 1994). The bath contained < 500 μl of saline and was continuously perifused at a rate of 2 ml/min using a gravity-driven perfusion system. The outflow was placed near the cell, resulting in complete solution exchange around the cell within 2 s. A solid Ag/AgCl reference electrode was connected to the bath via a 3 M KCl agar bridge.

Calculations. The time course of $[Ca^{2+}]_i$ response to ATP was fitted to one or two exponential functions using GraphPad Prism (GraphPad Software, San Diego, CA). All values in the text are reported as mean ± S.E.M. Significant differences, with $P < .05$, were determined by Student's t test.

Results

Ca^{2+} Signaling by Homomeric P2XRs. To examine Ca^{2+} signaling by recombinant P2XRs in excitable cells, the different P2XR subtypes were transiently expressed in GT1 neurons and the ATP-induced $[Ca^{2+}]_i$ response was monitored in single cells using fura-2 as a Ca^{2+} indicator. When the cells were stimulated with 100 μM ATP, all eight P2XR subtypes responded with a significant rise in $[Ca^{2+}]_i$ (Fig. 1A), whereas cells transfected with an empty vector did not respond (data not shown). The highest amplitude of $[Ca^{2+}]_i$ response to 100 μM ATP, expressed as mean values from 40 to 70 individual cells, was observed in $P2X_{2a}R$-expressing cells, followed by $P2X_{2b}R$-, $P2X_4R$-, $P2X_7R$-, $P2X_3R$-, and $P2X_1R$-expressing cells (Fig. 1B). $[Ca^{2+}]_i$ responses were also observed in $P2X_5R$- and $P2X_6R$-expressing cells, with a peak amplitude of 10 to 30% of that observed in $P2X_2R$-expressing cells. Because of their low and inconsistent $[Ca^{2+}]_i$ responses, $P2X_5R$ and $P2X_6R$ were not used in further studies.

Concentration-dependent studies revealed that no further increase in $[Ca^{2+}]_i$ was observed by increasing ATP concentration above 100 μM in cells expressing $P2X_1R$, $P2X_2R$, $P2X_3R$, and $P2X_4R$. That was not the case with $P2X_7R$-expressing cells in which a maximum $[Ca^{2+}]_i$ response was observed when stimulated with 1 mM ATP. Because of their low sensitivity to the native agonist, 3′*O*-(4-benzoyl)benzoyl-ATP (BzATP), a potent agonist for these channels, was also used in experiments. Furthermore, preincubation of cultures with apyrase, an ectoATPase, was necessary to detect changes in $[Ca^{2+}]_i$ in $P2X_1R$- and $P2X_3R$-expresssing cells, but not in cells expressing other P2XR subtypes. These results suggest that $P2X_1R$ and $P2X_3R$ are endogenously desensitized (i.e., that ATP concentrations spontaneously released by GT1 cells are sufficient to desensitize these but not other P2XRs). In all additional studies with these two channels, cells were incubated in apyrase-containing medium,

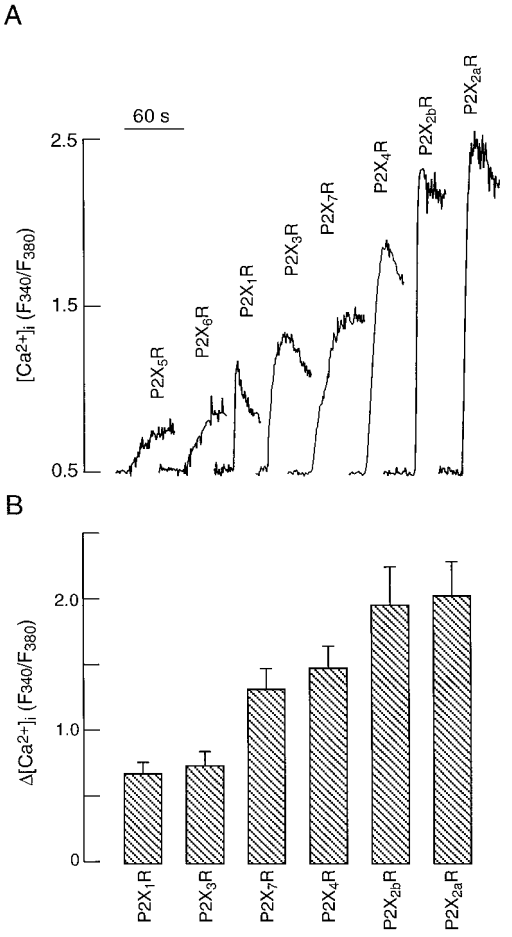

Fig. 1. Calcium signaling by homomeric P2XRs expressed in GT1 cells. A, representative tracings of 100 μM ATP-induced peak $[Ca^{2+}]_i$ responses. In these and the following experiments, cells were loaded with fura-2 and recordings were done in Ca^{2+}-containing Krebs-Ringer buffer, if not otherwise specified. B, averaged data of the peak $[Ca^{2+}]_i$ responses to 100 μM ATP (means ± S.E.M.) generated from at least 40 records per group. $[Ca^{2+}]_i$ was expressed as peak F_{340}/F_{380} subtracted by basal levels.

and $[Ca^{2+}]_i$ and electrophysiological recordings were also done in the presence of this compound.

Two reasons may underlie the observed differences in the amplitudes of $[Ca^{2+}]_i$ responses to high ATP concentration in cells expressing recombinant receptor-channels: the transfection and expression efficiency of these channels in common host cells, and/or the capability of these channels to promote Ca^{2+} influx. To analyze the potential impact of transfection and expression efficiency on the pattern of ATP-induced Ca^{2+} signaling, several different experimental approaches were employed. Initially, we estimated the amount of receptor protein in membrane fractions by Western blot analysis using a common anti-HA antibody, and compared it with the amplitude of $[Ca^{2+}]_i$ response. Adding an HA tag at the C-terminus did not alter receptor activity estimated in current and Ca^{2+} measurements (data not shown). The level of P2XR expression in GT1 cells was variable (Fig. 2A), indicating that each subunit shows a particular rate of protein production/degradation, even when expressed under the same transcriptional force by a CMV-promoter-based expression vector. Notably, the apparent amplitudes of averaged $[Ca^{2+}]_i$ response estimated in single cell $[Ca^{2+}]_i$ measurements (Fig. 1B) did not correlate with the protein amounts of subunits. For example, although the expression of $P2X_3R$ was the most effective, the averaged peak amplitude of $[Ca^{2+}]_i$ response was the lowest among channels compared. Furthermore, the expression of $P2X_{2a}R$, $P2X_{2b}R$, and $P2X_7R$ was comparable (Fig. 2A), but not their $[Ca^{2+}]_i$ responses when stimulated with 100 μM ATP (Fig. 1B). These findings indicate that the relative amount of receptors cannot account for the entire difference of the averaged peak amplitudes in $[Ca^{2+}]_i$ responses among P2XR types.

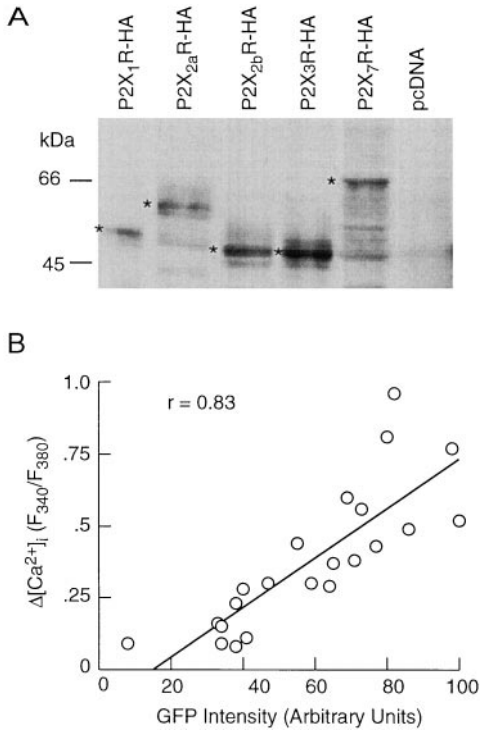

Fig. 2. Dependence of Ca^{2+} signaling by P2XRs on the efficiency of receptor expression. A, P2XRs having HA-tag at the C terminus were detected by Western blot analysis. Crude membrane fractions were prepared from transfected GT1 cells and used for SDS-PAGE as described under *Experimental Procedures*. Calculated molecular masses from blots were 58.3 kDa, 62.8 kDa, 51.8 kDa, 50.1 kDa, and 65.5 kDa for $P2X_1HA$, $P2X_{2a}HA$, $P2X_{2b}HA$, $P2X_3HA$, and $P2X_7HA$, respectively. These numbers are larger than expected molecular masses from their amino acid sequences, indicating expressed receptor proteins were glycosylated in GT1 cells. B, the relationship between GFP intensity and $[Ca^{2+}]_i$ response in cells expressing $P2X_3R$. The results shown are from a single experiment with simultaneous measurements of $[Ca^{2+}]_i$ in all cells expressing GFP, the intensity of which was recorded before $[Ca^{2+}]_i$ measurements. Cells were stimulated with 100 μM ATP. r, coefficient of correlation. Similar results were observed in three additional experiments.

In further studies, we compared the relative transfection efficiency of P2XRs construct in single cells by coexpressing GFP and P2XRs and analyzing the intensity of fluorescence signals as a measure of transfection efficiency. About 90% of GFP-expressing cells also responded to ATP, whereas only about 10% of GFP-negative cells responded to ATP. In the presence of fixed amount of the expression constructs, the percentage of GFP-ATP positive cells varied between 35 and 85%. It was independent on the channel type expressed and the method used for coexpression (see under *Experimental Procedures*). The GFP intensity varied among the cells in the same field, as well as the amplitude of ATP-induced $[Ca^{2+}]_i$ response. As illustrated in Fig. 2B, there was a linear correlation between the expression of GFP and the peak amplitude of $[Ca^{2+}]_i$ response in cells transiently transfected with $P2X_3R$. Such variation was not unique for $P2X_3R$, but was also observed in cells transfected with other channels. However, when the average GFP fluorescence was comparable for each set of cells (about 60 arbitrary units) (i.e., under similar transfection efficiency, the mean amplitude of $[Ca^{2+}]_i$ (F_{340}/F_{380}) response to 100 μM ATP (peak response − baseline) were 0.51 ± 0.04, 0.69 ± 0.08, 1.43 ± 0.16, 2.18 ± 0.21, and 2.29 ± 0.18 for $P2X_1R$, $P2X_3R$, $P2X_4R$, $P2X_{2a}R$, and $P2X_{2b}R$, respectively. These results again indicate that variations in the maximum $[Ca^{2+}]_i$ response were determined by the number of functional channels expressed in single cells, as well as by the capacity of channels to elevate $[Ca^{2+}]_i$ when stimulated with supramaximal agonist concentration.

We also generated cells stably expressing $P2X_1R$, $P2X_{2b}R$, or $P2X_{2a}R$ and analyzed their $[Ca^{2+}]_i$ responses. As shown in Fig. 3A, cell lines generated from single colonies exhibited variations in the peak $[Ca^{2+}]_i$ responses when stimulated with 100 μM ATP, but those were of a smaller magnitude than those observed in transiently transfected cells (Fig. 3A versus Fig. 4). The averaged peak amplitudes of $[Ca^{2+}]_i$ responses among these three receptors were significantly different (Fig. 4C) and comparable with those observed in cells coexpressing GFP and P2XRs (see above). We also examined the pattern of Ca^{2+} signaling in four different cells stably expressing $P2X_1R$. The peak $[Ca^{2+}]_i$ responses by these individual clones were comparable and were about 30% of that observed in cells expressing $P2X_{2b}R$ and $P2X_{2a}R$ (data not shown). These results indicate that the coexpression of P2XRs and GFP does not affect the ability of these channels to elevate $[Ca^{2+}]_i$ when activated and confirm the finding that Ca^{2+} signaling pattern by P2XRs is an intrinsic characteristic of these receptor-channels.

Characterization of Receptor Desensitization. We next compared the rates of receptor desensitization during sustained agonist stimulation and their dependence on the transfection and expression efficacy. Figure 4 illustrates typical tracings for P2XRs when recordings were done simultaneously in several cells in the field exhibiting different receptor expression. All P2XRs responded to ATP with a biphasic

increase in $[Ca^{2+}]_i$ that was composed of an initial spike response, followed by sustained steady-state plateau phase. P2XR subtypes differed in the relative amplitude of the plateau response and in the time needed to reach it; the latter reflects the desensitization rate. In $P2X_1R$- and $P2X_3R$-expressing cells, ATP-induced $[Ca^{2+}]_i$ response reached the plateau phase within 1 to 2 min of stimulation. $P2X_{2b}R$- and $P2X_4R$-derived $[Ca^{2+}]_i$ responses also decreased exponentially, reaching the low steady-state level within 2 to 4 min. On the other hand, application of ATP induced a long-lasting $[Ca^{2+}]_i$ response in cells expressing $P2X_{2a}R$ and $P2X_7R$. The $P2X_{2a}R$-induced $[Ca^{2+}]_i$ response decreased to one third of the maximum response within 10 min of stimulation. In the $P2X_7R$-expressing cells stimulated with 100 μM BzATP, no obvious desensitization was observed during the first 10 min of stimulation (Fig. 4).

In contrast to the amplitude of $[Ca^{2+}]_i$ response, the rate of receptor desensitization was independent on the levels of receptor expression. The numbers below the traces shown in Fig. 4 indicate the rates of receptor desensitization derived from the fitted curves (full lines) in cells exhibiting different level of P2XR expression. When stimulated with 100 μM ATP, the mean rates of desensitization were (in s^{-1}) 0.041 $\pm$ 0.004 (n = 54) for $P2X_3R$; 0.034 $\pm$ 0.004 (n = 43) for $P2X_1R$; 0.022 $\pm$ 0.006 (n = 57) $P2X_{2b}R$; 0.017 $\pm$ 0.001 (n = 34) for $P2X_4R$; and 0.006 $\pm$ 0.0004 (n = 58) for $P2X_{2a}R$. Because $P2X_7R$-expressing cells showed no obvious desensitization of $[Ca^{2+}]_i$ response when stimulated with 100 μM BzATP, the rates of desensitization were not calculated.

The receptor-specific desensitization rates were also observed in stably transfected cells. As shown in Fig. 3B, there was a significant difference in the rate of desensitization between $P2X_1R$ and $P2X_{2a}R/P2X_{2b}R$, as well as between $P2X_{2a}R$ and $P2X_{2b}R$ when cells were stimulated with 100 μM ATP. The average rates of receptor desensitization derived from these experiments were comparable with those derived from the transiently transfected cells. These results further indicate that the rate of P2XRs desensitization is an intrinsic and unique feature of a particular receptor and is not affected by the level of protein expression.

Relationship between $[Ca^{2+}]_i$ and Current Responses in P2XR-Expressing Cells. In parallel to $[Ca^{2+}]_i$ measurements, ATP-induced currents were measured using perforated patch-recording techniques. For this purpose,

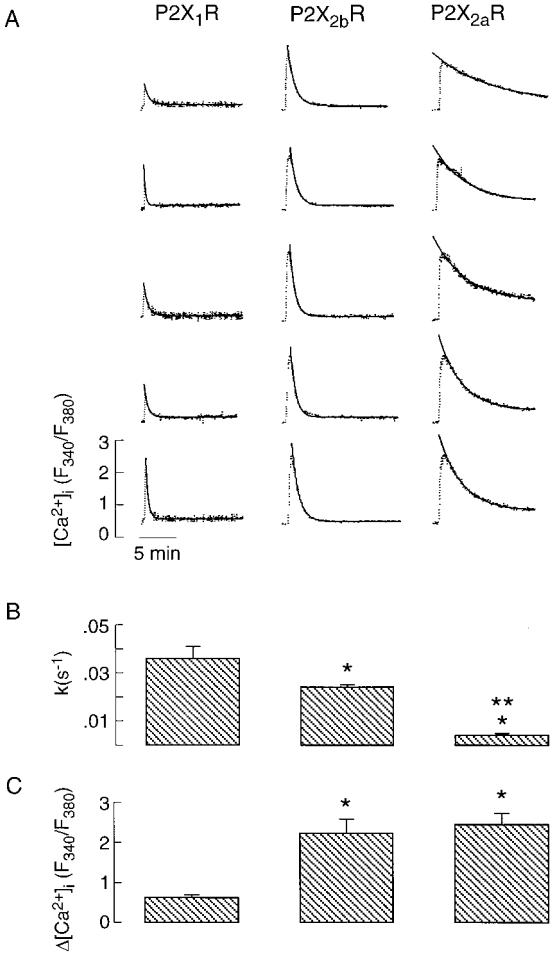

Fig. 3. Pattern of Ca^{2+} signaling by P2XR stably expressing in GT1 neurons. A, representative tracings (dotted lines) and fitted curves (solid lines) of 100 μM ATP-induced $[Ca^{2+}]_i$ signals in $P2X_1R$-, $P2X_{2b}R$-, and $P2X_{2a}R$-expressing cells. B and C, the calculated rates of receptor desensitization (B) and peak amplitude $[Ca^{2+}]_i$ responses (C). The bars shown are means $\pm$ S.E.M. derived from at least 15 records. * $P < .05$ versus $P2X_1R$; ** $P < .05$ versus $P2X_{2b}R$.

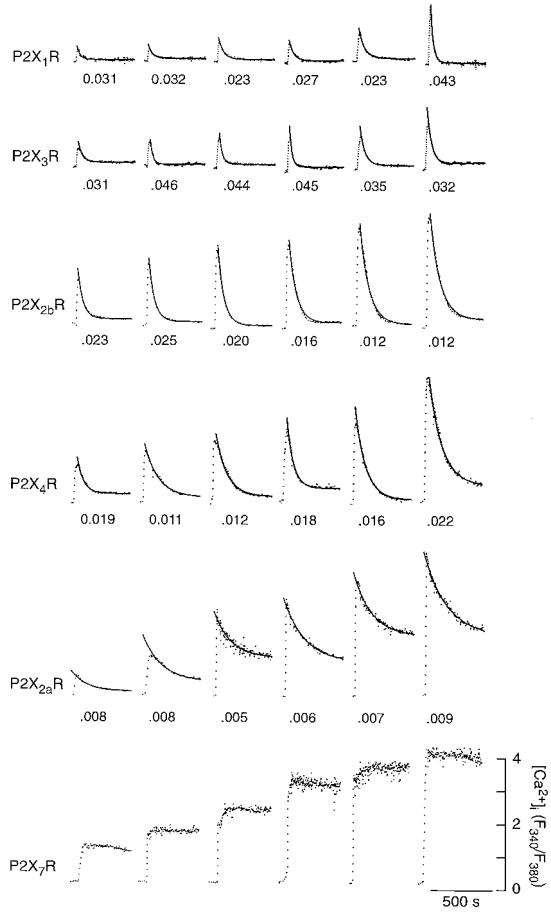

Fig. 4. Pattern of Ca^{2+} signals by P2XRs transiently expressed in GT1 neurons. The tracings shown by dotted lines are derived from the single recording for each receptor and are illustrative for the variations among cells expressing a particular receptor. Cells were stimulated with 100 μM ATP, or with 100 μM BzATP when $P2X_7Rs$ were analyzed. In all tracings, single exponential functions were sufficient to describe the desensitization (solid lines). The fitted function is extrapolated for clarity. The calculated desensitization constants are shown below the tracings. X and Y scales shown in the right bottom corner are common for all tracings shown.

cells expressing homomeric P2XRs were given 100 μM ATP, whereas $P2X_7R$-expressing cells received 500 μM ATP. To exclude the participation of voltage-sensitive Ca^{2+} influx to the ATP-induced $[Ca^{2+}]_i$ response, cells were clamped at a holding potential of −90 mV. Activation of all recombinant channels evoked an inward current, the pattern of which was unique to each receptor subtype with respect to its desensitization rate (Fig. 5). The rank orders of the current amplitude and desensitization rate were highly comparable with those observed in $[Ca^{2+}]_i$ measurements, suggesting that the pattern of Ca^{2+} signaling by recombinant receptors is determined by the pattern of depolarizing current. Thus, when expressed in an excitable cell, both current and $[Ca^{2+}]_i$ responses can be used to study receptor activation and desensitization.

In further experiments, we simultaneously monitored ATP-induced current and $[Ca^{2+}]_i$ responses to ATP in indo-1-loaded cells expressing $P2X_3R$ and $P2X_{2b}R$. Activation of both receptors generated currents with profiles highly comparable with those observed in cells without dye (Fig. 6 versus Fig. 5). Thus, loading the cells with Ca^{2+} indicator dye does not affect the pattern of the current response. However, clamping the cells at −90 mV significantly altered the profile of the $[Ca^{2+}]_i$ response. In clamped cells, only a low-amplitude monophasic $[Ca^{2+}]_i$ response accompanied the ATP-induced current in $P2X_3R$-expressing cells (Fig. 6A, upper tracing), in contrast, in unpatched cells expressing $P2X_3R$, which responded to ATP with a biphasic $[Ca^{2+}]_i$ profile (Fig. 3). These results indicate that clamping the cells at −90 mV effectively abolishes the spike $[Ca^{2+}]_i$ response in $P2X_3R$-expresssing cells. This suggests that voltage-sensitive Ca^{2+} influx is the major pathway contributing to the peak rise in $[Ca^{2+}]_i$ in $P2X_3R$-expressing cells.

In contrast to $P2X_3R$-expresssing cells, $P2X_{2b}R$-expressing cells responded to ATP when clamped at −90 mV with a pattern of $[Ca^{2+}]_i$ response that was comparable with those observed in unpatched cells (Fig. 6B versus Figs. 3 and 4). These results indicate that $P2X_{2b}R$ can generate biphasic Ca^{2+} signals when voltage-sensitive Ca^{2+} influx is blocked. Our measurements also confirmed that the time course for the activation and desensitization of ATP-induced current and $[Ca^{2+}]_i$ responses significantly differ when measured simultaneously in the same cells (see Fig. 6 legend) [i.e., that desensitization of the $[Ca^{2+}]_i$ response occurred with 43 ± 12 s delay (n = 5) compared with the current response (indicated by arrows in Fig. 6B)]. Because voltage-sensitive Ca^{2+} influx was blocked by clamping the cells at −90 mV, the Ca^{2+} handling mechanism of the cells seemed to be a major factor contributing to the delay in decrease of $[Ca^{2+}]_i$ during continuous agonist stimulation.

Dependence of $[Ca^{2+}]_i$ Response on Voltage-Sensitive and -Insensitive Ca^{2+} Influx. To examine the impact of voltage-sensitive Ca^{2+} entry on ATP-induced $[Ca^{2+}]_i$ response in more detail, GT1 neurons expressing $P2X_1R$, $P2X_3R$, $P2X_4R$, $P2X_{2a}R$, $P2X_{2b}R$, and $P2X_7R$ were bathed in medium containing 1 μM nifedipine, a blocker of L-type

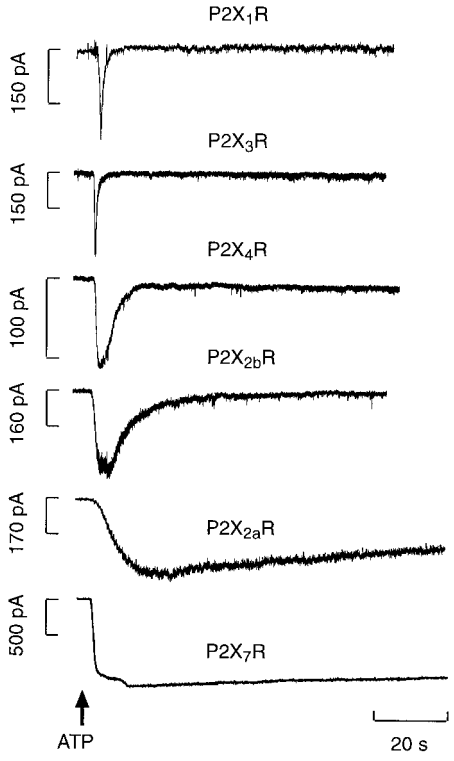

Fig. 5. ATP-induced inward current in GT1 cells expressing recombinant P2XRs. The $P2X_7R$-expressing cells were stimulated with 500 μM ATP, whereas all other receptor-expressing cells were stimulated with 100 μM ATP. Note the differences in the amplitudes of current responses (variable Y-axes). All recordings were done in cells clamped at −90 mV and bathed in Ca^{2+}-containing medium.

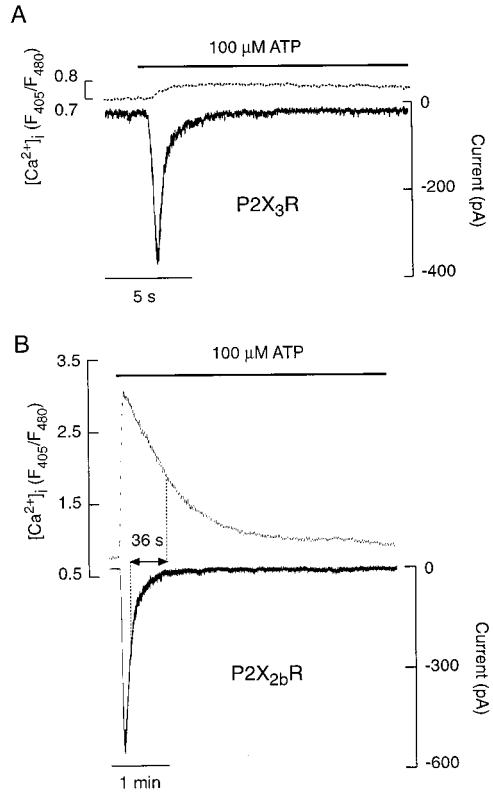

Fig. 6. ATP-induced calcium and current signaling in $P2X_{2b}R$- and $P2X_3R$-expresssing cells. A, simultaneous measurements of current and $[Ca^{2+}]_i$ in $P2X_3R$-expresssing cells. B, pattern of ATP-induced current and $[Ca^{2+}]_i$ response in GT1 cells expressing $P2X_{2b}R$. The half-times for desensitization of current and $[Ca^{2+}]_i$ responses were 11.90 ± 1.34 s (n = 5) and 54.92 ± 12.37 s (n = 5; $P < .015$). To exclude the participation of voltage-sensitive Ca^{2+} entry, the cells were clamped at −90 mV. In these experiments, cells were loaded with indo-1 and stimulated with 100 μM ATP. Note the difference in time-scales between the two experiments.

calcium channels, and $[Ca^{2+}]_i$ was monitored in unpatched cells. As shown in Fig. 7A, GT1 neurons exhibit spontaneous firing of action potential that controls basal $[Ca^{2+}]_i$. Addition of nifedipine abolished electrical activity and decreased $[Ca^{2+}]_i$.

In cells expressing $P2X_3R$, ATP induced a small monophasic $[Ca^{2+}]_i$ response in nifedipine-containing medium. The profile of $[Ca^{2+}]_i$ response was similar to that observed in voltage-clamped cells (Figs. 6A and 7B, tracing *b*). Nifedipine also abolished the spike $[Ca^{2+}]_i$ response in $P2X_1R$- and $P2X_4R$-expressing cells (tracings a and c) but not in $P2X_{2a}R$- and $P2X_{2b}R$-expressing cells. As shown in Fig. 7B, d and e, both spike and plateau responses were observed in nifedipine-treated cells, but the amplitudes of these responses were reduced.

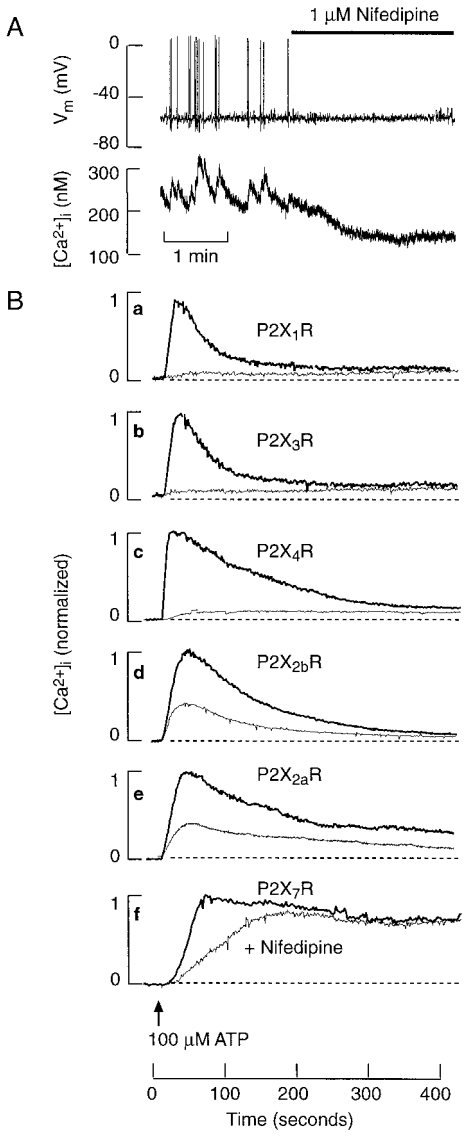

Fig. 7. Nifedipine-sensitivity of ATP-induced $[Ca^{2+}]_i$ responses. A, effects of nifedipine on spontaneous electrical activity and $[Ca^{2+}]_i$ in GT1 neurons. Electrical activity and $[Ca^{2+}]_i$ were recorded simultaneously in indo-1 loaded cells. B, averaged tracings of $[Ca^{2+}]_i$ profile (n = 10) in controls (thick lines) and cells bathed in 1 μM nifedipine-containing medium (thin lines). The amplitudes of $[Ca^{2+}]_i$ responses were normalized (Y axes). Dashed lines illustrate the baseline $[Ca^{2+}]_i$. The averaged data on the effects of nifedipine on the peak $[Ca^{2+}]_i$ responses are shown in Table 1. $[Ca^{2+}]_i$ was recorded in fura-2-loaded cells.

The dependence of Ca^{2+} signaling by $P2X_7R$ on voltage-sensitive Ca^{2+} influx was more complex than that observed in $P2X_2R$-expressing cells. A nifedipine-sensitive component in $[Ca^{2+}]_i$ response was consistently observed, but only during the early phase of stimulation with lower concentrations of ATP. As shown in Fig. 7B, tracing f, the rise in $[Ca^{2+}]_i$ in response to 100 μM ATP was delayed, but not reduced, in nifedipine-treated cells, and there was no difference in the amplitude of the plateau responses in controls and treated cells 200 s after the addition of ATP. Similarly, the rise in $[Ca^{2+}]_i$ was delayed in nifedipine-treated cells stimulated with 500 μM ATP, but these cells frequently showed a secondary elevation in $[Ca^{2+}]_i$ (Fig. 8A, right tracing). The amplitude of $[Ca^{2+}]_i$ response during the second phase reached that observed in cells stimulated with BzATP, a selective and highly potent agonist for $P2X_7R$. The $[Ca^{2+}]_i$ response to BzATP was nifedipine-insensitive (Fig. 8, left tracings). Finally, $P2X_7R$-expressing cells responded to 1 mM ATP by a rise in $[Ca^{2+}]_i$ with a pattern indistinguishable from that observed in 100 μM BzATP-stimulated cells and unaffected by nifedipine (data not shown). In some cells, we also observed the third phase in activation of $P2X_7R$. GT1 neurons stimulated with 100 μM BzATP were permeabilized after prolonged (10 to 20 min) stimulation, in which $[Ca^{2+}]_i$ mea-

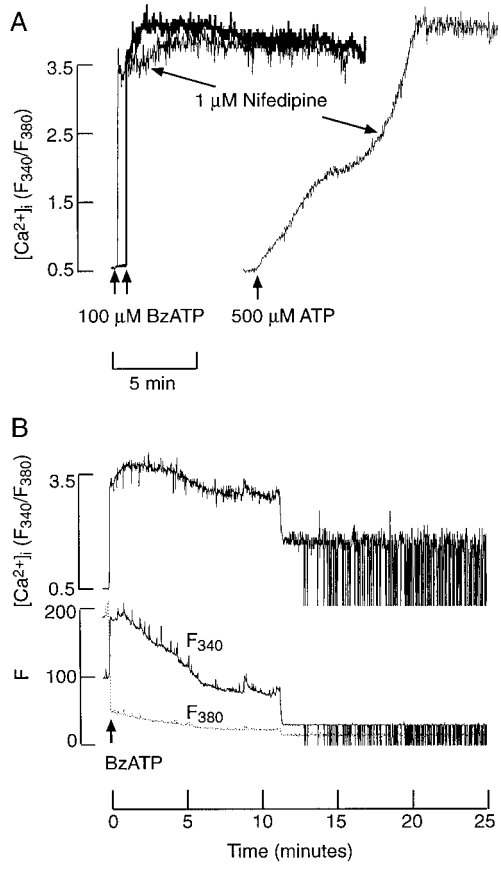

Fig. 8. Calcium signaling by $P2X_7R$. A, independence of agonist-induced $[Ca^{2+}]_i$ response on Ca^{2+} influx through L-type voltage-gated calcium channels. Thick line illustrates the pattern of $[Ca^{2+}]_i$ response in BzATP-stimulated cells bathed in medium without nifedipine. B, permeabilization of cells, indicated by the leak of fura-2. This effect was occasionally observed in BzATP-stimulated cells expressing $P2X_7R$, but only during prolonged stimulation.

surements were affected by the leak of fura-2 from cells (Fig. 8B).

The effects of nifedipine on $[Ca^{2+}]_i$ responses by recombinant receptors are summarized in Table 1. The peak $[Ca^{2+}]_i$ response was significantly affected in $P2X_1R$-, $P2X_3R$-, $P2X_4R$-, $P2X_{2a}R$-, and $P2X_{2b}R$-expresssing cells, but not in $P2X_7R$-expresssing cells. The nifedipine-insensitive $[Ca^{2+}]_i$ response was 7, 8, 13, 46, 47, and 96% in cells expressing $P2X_1R$, $P2X_3R$, $P2X_4R$, $P2X_{2a}R$, $P2X_{2b}R$, and $P2X_7R$, respectively. Thus, Ca^{2+} signaling by all P2XRs was to some extent dependent on both voltage-insensitive and -sensitive Ca^{2+} influx. Calcium signaling by $P2X_1R$, $P2X_3R$, and $P2X_4R$ was critically dependent on voltage-sensitive Ca^{2+} influx, whereas both pathways equally contributed to $[Ca^{2+}]_i$ responses in $P2X_{2a}R$- and $P2X_{2b}R$-expressing cells. Activation of $P2X_7R$ also led to the facilitated voltage-sensitive Ca^{2+} influx, but only transiently and when cells were stimulated with lower ATP concentrations. The inefficacy of nifedipine at supramaximal concentrations and the high amplitude of current/$[Ca^{2+}]_i$ responses indicated that this channel operates as a nonselective pore capable of conducting larger amounts of Ca^{2+} independently on the status of voltage-gated Ca^{2+} channels.

Relationship between Voltage-Sensitive and Voltage-Insensitive Ca^{2+} Influx. To further analyze the relationship between voltage-sensitive and voltage-insensitive Ca^{2+} influx in activated receptors, we chose $P2X_2R$-expressing cells, because of the significant contribution of both pathways to the ATP-induced $[Ca^{2+}]_i$ response. The dependence of voltage-sensitive Ca^{2+} influx on the pattern of current response was studied in unloaded and indo-1-loaded cells. In both experiments, we initially recorded the pattern of spontaneous V_m before and during ATP stimulation in the current-clamp recording mode. The cells were then washed for 10 min to allow for recovery from desensitization (Koshimizu et al., 1998b) and clamped to −90 mV in the voltage-clamp recording mode, and restimulated with 100 μM ATP to measure the current response. In indo-1-loaded cells, the $[Ca^{2+}]_i$ and V_m were recorded simultaneously during the initial stimulation and measurement of current was performed during the second ATP stimulation.

Figure 9A illustrates the V_m response measured in two unloaded GT1 cells expressing $P2X_{2b}R$, one responding to ATP with a small (15 pA) peak amplitude current (left tracings) and the other responding to ATP with higher (180 pA) peak amplitude current (right tracings). In both cells, the peak current response coincided with the highest frequency of firing, and the desensitization rate of current response paralleled the normalization of firing frequency. The average frequency of spiking was higher in the cell generating current of higher amplitude. A similar dependence of the pattern of firing on the size of the depolarizing current and the rate of current desensitization was observed in indo-1-loaded cells (Fig. 9B). Simultaneous measurements of V_m and $[Ca^{2+}]_i$ responses also revealed that the frequency of spiking encodes ATP-induced voltage-gated Ca^{2+} influx.

To examine whether voltage-sensitive Ca^{2+} influx can alter the desensitization rate of ATP-induced $[Ca^{2+}]_i$ responses, $P2X_{2a}R$- and $P2X_{2b}R$-expressing cells bathed in medium with or without nifedipine were stimulated with 100 μM ATP. The tracings shown in Fig. 10 (dotted lines) are representative of 15 records for both receptors and each group (with and without nifedipine). The peak amplitude of $[Ca^{2+}]_i$ response was significantly reduced in the presence of nifedipine, but the rate of Ca^{2+} signal desensitization was not affected, as indicated by the parallelism in the fitted curves (full lines) and the mean values for the calculated rates of desensitization, shown on right. These results indicate that despite amplifying ATP-induced Ca^{2+} signals, voltage-sensitive Ca^{2+} influx does not affect the rate of receptor desensitization.

TABLE 1

Dependence of the peak $[Ca^{2+}]_i$ response to ATP on voltage-sensitive and -insensitive Ca^{2+} influx in cells expressing recombinant receptors

Cells were stimulated with 100 μM ATP or 100 μM BzATP (bottom value).

Receptor Subtype	Controls	Nifedipine-Treated
$P2X_1R$ (ATP)	0.56 ± 0.07[a]	0.04 ± 0.01*
$P2X_3R$ (ATP)	0.85 ± 0.12	0.07 ± 0.01*
$P2X_4R$ (ATP)	1.29 ± 0.14	0.18 ± 0.03*
$P2X_{2a}R$ (ATP)	2.03 ± 0.25	0.95 ± 0.11*
$P2X_{2b}R$ (ATP)	1.97 ± 0.19	0.93 ± 0.13*
$P2X_7R$ (ATP)	0.98 ± 0.13	0.94 ± 0.08
$P2X_7R$ (BzATP)	3.45 ± 0.53	3.39 ± 0.61

[a]Data shown are $[Ca^{2+}]_i$, expressed as peak F_{340}/F_{380} subtracted by basal levels.
* $P < .01$ versus control.

Discussion

In this study, we compared the ability of recombinant P2XRs to initiate and sustain current and Ca^{2+} signaling. For this purpose, we used immortalized GT1 neurons, which do not express ATP-gated receptors or receptor-channels (Ko-

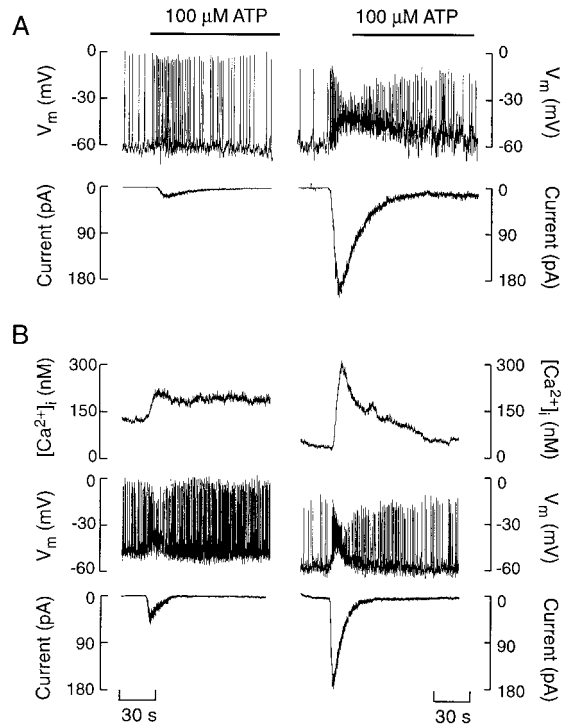

Fig. 9. Modulation of electrical activity by activated $P2X_{2b}R$ in spontaneously firing GT1 neurons. A, two examples of ATP-induced changes in the firing pattern in GT1 cells. Notice the difference in the amplitude of inward currents on the left and right tracings. B, simultaneous measurement of V_m and $[Ca^{2+}]_i$, in ATP-stimulated cells. In A and B, cells expressing $P2X_{2b}R$ were initially stimulated with 100 μM ATP for V_m recordings, and then washed for 10 min and restimulated with 100 μM ATP to measure the current amplitude in cells clamped at −90 mV.

shimizu et al., 1998b), in contrast to many other immortalized cells commonly used in transfection studies. GT1 neurons express T- and L-type voltage-gated Ca^{2+} channels and spontaneously fire nifedipine-sensitive action potentials (Van Goor et al., 1999a,b). This makes them an excellent cell model for studying the participation of voltage-gated Ca^{2+} influx in response to activation of P2XRs. This is of the physiological relevance, because P2XRs are expressed in many excitable cell types and participate in the control of synaptic transmission and neurosecretion (Brake and Julius, 1996).

When expressed individually in GT1 cells, all eight types of P2XRs studied responded to ATP with a significant rise in $[Ca^{2+}]_i$, but with variable patterns of calcium signaling. Ca^{2+} influx by $P2X_1R$, $P2X_3R$, and $P2X_4R$ was predominantly mediated through depolarization of cells and activation of voltage-sensitive Ca^{2+} influx, whereas both Ca^{2+} influx through the pore of channels and voltage-sensitive Ca^{2+} influx participated in the $[Ca^{2+}]_i$ responses of $P2X_{2a}R$ and $P2X_{2b}R$. Activation of $P2X_7R$ also led to facilitation of voltage-sensitive Ca^{2+} influx, but only transiently. These novel observations suggest that all P2XR studied operate as bifunctional molecules when expressed in excitable cells; they conduct Ca^{2+} and promote voltage-sensitive Ca^{2+} influx.

Both current amplitude and its rate of desensitization affect Ca^{2+} influx through the pore of recombinant receptors and through voltage-gated Ca^{2+} channels, doing the latter by encoding the frequency of action potential firing. ATP-induced current in $P2X_1R$-, $P2X_3R$-, and $P2X_4R$-expressing cells rapidly desensitized and the small amplitude $[Ca^{2+}]_i$ response observed in cells with blocked voltage-sensitive

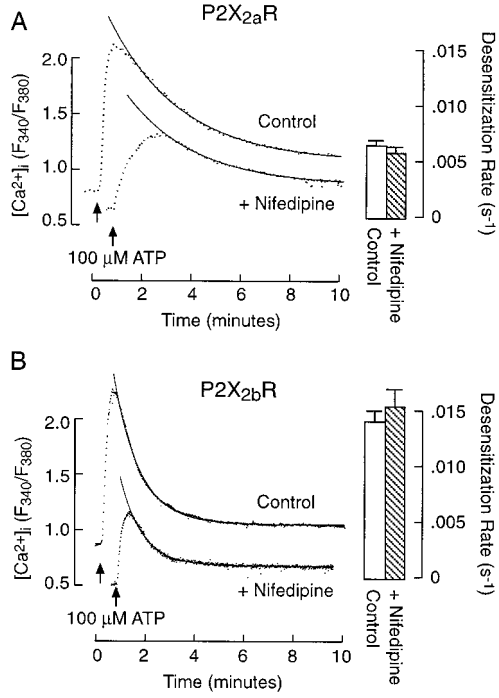

Fig. 10. Independence of receptor desensitization on voltage-sensitive calcium influx. Desensitization of $P2X_{2a}R$ (A) and $P2X_{2b}R$ (B) derived from $[Ca^{2+}]_i$ responses in controls and cells bathed in the presence of nifedipine. In both experiments, a single exponential function was sufficient to describe the desensitization (solid lines). The fitted function is extrapolated for clarity. The calculated desensitization constants are shown on the right, with $n = 15$ for all groups.

Ca^{2+} influx coincided with the steady-state current. On the other hand, the half-times of $P2X_{2a}R$ and $P2X_{2b}R$ current desensitization were prolonged compared with $P2X_1R$, $P2X_3R$, and $P2X_4R$, a time-frame sufficient to generate high amplitude $[Ca^{2+}]_i$ signals through the pore of receptors. Thus, although $P2X_1R$ and $P2X_2R$ exhibit similar conductivity for Ca^{2+} versus Na^+ (Evans et al., 1996), the ability of the first receptor to generate Ca^{2+} signal in cells under a block of voltage-gated Ca^{2+} influx is limited by its rapid desensitization.

The pattern of $[Ca^{2+}]_i$ signals generated by homomeric P2XRs in cells without the blockade of voltage-sensitive Ca^{2+} influx resembled that of current signaling. Current and Ca^{2+} signals desensitized with rates characteristic to each receptor subtype: $P2X_3R > P2X_1R > P2X_{2b}R > P2X_4R \gg P2X_{2a}R \gg P2X_7R$. Similar order was observed in current measurements in *X. laevis* oocytes expressing homomeric P2XRs (Evans et al., 1997). However, times needed to reach the steady desensitized states for P2XRs were significantly longer in Ca^{2+} than in current measurements. Simultaneous $[Ca^{2+}]_i$ and current measurements in $P2X_{2b}R$-expressing cells suggest that a delay in Ca^{2+} signal desensitization reflects the slow kinetics of Ca^{2+} elimination from the cytoplasm. Thus, $[Ca^{2+}]_i$ recordings are of limited use for studies on dynamics of channel behavior, but they can be effectively employed as an indicator of receptor desensitization when expressed in an excitable cell.

The P2XRs also differed among themselves with respect to endogenous desensitization. $P2X_1R$ and $P2X_3R$ were able to initiate measurable Ca^{2+} signals, but only in the presence of apyrase. When expressed in GT1 neurons, as in other cell types, the activity of this receptor is critically dependent on the level of ectoATPase activity (Edwards et al., 1992; MacKenzie et al., 1996). The need for apyrase indicates that spontaneous release or pathological leakage of ATP is of sufficient magnitude to desensitize $P2X_1R$ and $P2X_3R$ though not other members of P2XRs. Consistent with this hypothesis, concentration-dependent studies revealed that lower concentrations of ATP were required to reach the peak $[Ca^{2+}]_i$ responses by $P2X_1R$ and $P2X_3R$, compared with $P2X_{2a}R$, $P2X_{2b}R$, and $P2X_4R$.

In accordance with the literature in other cell types (Rassendren et al., 1997), $P2X_7R$ expressed in GT1 cells exhibited several unique features compared with other P2XRs. This receptor is the least sensitive to ATP among P2XRs. At lower ATP concentrations, the channel conducts Ca^{2+} and activates voltage-sensitive Ca^{2+} influx. The lack of effects of nifedipine at supramaximal agonist concentrations and the sizes of current and $[Ca^{2+}]_i$ responses indicate that this channel also operates as a nonselective pore capable of providing a massive Ca^{2+} influx. Ultimately, prolonged agonist stimulation of $P2X_7R$-expressing cells leads to cell permeabilization. Thus, $P2X_7R$ operates as a multifunctional receptor-channel. Because of the extremely high ATP concentrations needed to fully activate these channels, it is difficult to speculate on the physiological relevance of the transition from selective to nonselective pores and their permeability to larger molecules.

In conclusion, our results indicate that all recombinant P2XRs studied can generate Ca^{2+} signals when expressed as homomers in an excitable cell. The pattern of Ca^{2+} signaling

is unique to each receptor with respect to the EC_{50} for ATP, the amplitude and duration of current/$[Ca^{2+}]_i$ responses, and the dependence of $[Ca^{2+}]_i$ response on voltage-sensitive Ca^{2+} influx. Such specificity is of the potential physiological relevance because it provides an effective mechanism for generating variable $[Ca^{2+}]_i$ patterns in response to a common agonist.

References

Barry PH (1994) JPCalc, a software package for calculating liquid junction potential corrections in patch-clamp, intracellular, epithelial and bilayer measurements. *J Neurosci Methods* **51:**107–116.

Bo X, Zhang Y, Nassar M, Burnstock G and Schoepfer R (1995) A P2X purinoreceptor cDNA conferring a novel pharmacological profile. *FEBS Lett* **375:**129–133.

Brake AJ and Julius D (1996) Signaling by extracellular nucleotides. *Annu Rev Cell Dev Biol* **12:**519–541.

Brake AJ, Wagenbach MJ and Julius D (1994) New structural motif for ligand-gated ion channels defined by an ionotropic ATP receptor. *Nature (Lond)* **371:**519–523.

Brandle U, Spielmanns P, Osteroth R, Sim J, Surprenant A, Buell G, Ruppersberg JP, Plinkert PK, Zenner HP and Glowatzki E (1997) Desensitization of the $P2X_2$ receptor controlled by alternative splicing. *FEBS Lett* **404:**294–298.

Buell G, Collo G and Rassendren F (1996) P2X Receptors: An emerging channel family. *Eur J Neurosci* **8:**2221–2228.

Chen C-C, Akoplan AN, Sivllott L, Colquhoun D, Burnstock G and Wood JN (1995) A P2X purinoreceptor expressed by a subset of sensory neurons. *Nature (Lond)* **377:**428–431.

Collo G, North RA, Kawashima E, Merlo-Pich E, Neidhart S, Surprenant A and Buell G (1996) Cloning of $P2X_5$ and $P2X_6$ receptors and the distribution and properties of an extended family of ATP-gated ion channels. *J Neurosci* **16:**2495–2507.

Edwards FA, Gibb AJ and Colquhoun D (1992) ATP receptor-mediated synaptic currents in the central nervous system. *Nature (Lond)* **359:**144–147.

Evans RJ, Lewis C, Virginio C, Lundstrom K, Buell G, Surprenant A and North RA (1996) Ionic permeability of, and divalent cation effects on, two ATP-gated cation channels (P2X receptors) expressed in mammalian cells. *J Physiol* **497:**413–422.

Evans RJ, Surprenant A and North RA (1997) P2X receptors: Cloned and expressed, in *The P2 Nucleotide Receptors* (Turner JT, Weisman GA, and Fedan JS eds) pp 43, Humana Press Inc., Totowa, New Jersey.

Garcia-Guzman M, Soto F, Laube B and Stuhmer W (1996) Molecular cloning and functional expression of a novel rat heart P2X purinoreceptor. *FEBS Lett* **338:**123–127.

Hille B (1991) Ionic channels of excitable membranes. Sinauer Associates Inc., Sunderland, Massachusetts.

Koshimizu T, Koshimizu M and Stojilkovic S (1999) Contributions of the C-terminal domain to the control of P2X receptor desensitization. *J Biol Chem* **274:**37651–37657.

Koshimizu T, Tomic M, Koshimizu M and Stojilkovic SS (1998a) Identification of amino acid residues contributing to desensitization of the $P2X_2$ receptor channel. *J Biol Chem* **273:**12853–12857.

Koshimizu T, Tomic M, Van Goor F and Stojilkovic SS (1998b) Functional role of alternative splicing in pituitary $P2X_2$ receptor-channel activation and desensitization. *Mol Endocrinol* **12:**901–913.

Lewis C, Neidhart S, Holy C, North RA, Buell G and Surprenant A (1995) Coexpression of $P2X_2$ and $P2X_3$ receptor subunits can account for ATP-gated currents in sensory neurons. *Nature (Lond)* **377:**432–435.

MacKenzie AB, Mahaut-Smith MP and Sage SO (1996) Activation of receptor-operated cation channels via $P2X_1$ not P_{2T} purinoreceptors in human platelets. *J Biol Chem* **271:**2879–2881.

North RA (1996) P2X receptors: A third major class of ligand-gated ion channels. *Ciba Found Symp* **198:**91–105.

Rae J, Cooper K, Gates P and Watsky M (1991) Low access resistance perforated patch recordings using amphotericin B. *J Neurosci Methods* **37:**15–26.

Ralevic V and Burnstock G (1998) Receptors for purines and pyrimidines. *Pharmacol Rev* **50:**413–492.

Rassendren F, Buell GN, Virginio C, Collo G, North A and Surprenant A (1997) The permeabilizing ATP receptor, $P2X_7$. *J Biol Chem* **272:**5482–5486.

Soto F, Garcia-Guzman M, Gomez-Hernandez JM, Hollmann M, Karschin C and Stuhmer W (1996) P2X4: An ATP-activated ionotropic receptor cloned from rat brain. *Proc Natl Acad Sci USA* **93:**3684–3688.

Van Goor F, Krsmanovic LZ, Catt KJ and Stojilkovic SS (1999a) Control of action potential-driven calcium influx in GT1 neurons by the activation status of sodium and calcium channels. *Mol Endocrinol* **13:**587–603.

Van Goor F, Krsmanovic LZ, Catt KJ and Stojilkovic SS (1999b) Coordinate regulation of gonadotropin-releasing hormone neuronal firing patterns by cytosolic calcium and store depletion. *Proc Natl Acad Sci USA* **96:**4101–4106

Send reprint requests to: Dr. Stanko Stojilkovic, Section on Cellular Signaling, ERRB/NICHD/NIH, Bldg. 49, Room 6A-36, 49 Convent Drive, Bethesda, MD 20892. E-mail: stankos@helix.nih.gov